PAPER

An Edge-Preserving Super-Precision for Simultaneous Enhancement of Spacial and Grayscale Resolutions

Hiroshi HASEGAWA[†a)], ***Member***, **Toshinori OHTSUKA**[††], ***Nonmember***, **Isao YAMADA**[††], ***Member***, ***and*** **Kohichi SAKANIWA**[††], ***Fellow***

SUMMARY In this paper, we propose a method that recovers a smooth high-resolution image from several blurred and roughly quantized low-resolution images. For compensation of the quantization effect we introduce measurements of smoothness, Huber function that is originally used for suppression of block noises in a JPEG compressed image [Schultz & Stevenson '94] and a smoothed version of total variation. With a simple operator that approximates the convex projection onto constraint set defined for each quantized image [Hasegawa et al. '05], we propose a method that minimizes these cost functions, which are smooth convex functions, over the intersection of all constraint sets, i.e. the set of all images satisfying all quantization constraints simultaneously, by using hybrid steepest descent method [Yamada & Ogura '04]. Finally in the numerical example we compare images derived by the proposed method, Projections Onto Convex Sets (POCS) based conventinal method, and generalized proposed method minimizing energy of output of Laplacian.

key words: *super-resolution, Huber function, total variation, set-theoretic approach, outer approximation, hybrid steepest descent method*

1. Introduction

A great deal of effort has been devoted to derive a high-resolution image from degraded low-resolution images having potential redundancy [1], [2]. Such a technique is called *super-resolution* and its application ranges from HDTV to satellite/medical imaging.

Recently several challenges are shown to improve not only the spacial resolution but also precision of each pixel, namely *bit-depth*. In this paper, we call techniques to tackle such a problem *super-precision*. Gunturk et al. demonstrated that it is possible to compensate the effect of rough quantization by using multiple images [3]. On the other hand, super-resolution of MPEG video [4]–[6] is also an example of the super-precision, because it is nothing but the compensation of quantization error in the MPEG compression that consists of rough quantization after subtraction of known vector, called motion compensation, and an orthogonal transform, i.e. discrete cosine transform. These recovery techniques would potentially improve compression of high-resolution videos.

Since the quantization constraint leads to numerous linear inequalities and the recovered image is large in general for super-resolution, simple iterative scheme to derive a solution is desirable. Indeed, conventional methods search for an image satisfying all given quantization conditions [3], [4] by Projections Onto Convex Sets (POCS) [7], that consists of sequential convex projections onto half spaces defined by these inequalities. The other approach [6] modifies the original problem to an unconstrained maximization of the multidimensional Gaussian function, which approximates the quantization error, so that a simple scheme such as a steepest descent method resolves the problem. However, the set of all candidates for the solutions is generally broad because the quantization interval would be large for higher compression rates. In such a case, one of the most natural approaches would be finding a visually natural image among the set of all images satisfying given quantization constraints. Indeed, ML-POCS [8] provides such a image by iterative convex projections onto a convex set satisfying all of given constraints, that is defined by low resolution images and additive noise and essentially equivalent to the quantization constraints, and update to steepest descent directions. However, the proof in [8] only guarantees convergence to the optimal solution only if the convex projection onto a convex set, in which each image satisfies all constraints simultaneously, can be computed, although the computation is difficult in general because the set has complicated shape when different blur and shift parameters are assumed.

In this paper, we propose a method that pursuits a smooth high-resolution image among the set of all possible candidates defined by differently blurred and roughly quantized low-resolution images. To derive a smooth image while keeping the edge information, we introduce differentiable functions, Huber function [9], [10] and a smoothed version of total variation, where the former had been successfully applied for suppression of block noises in a JPEG compressed image [9]. By combining hybrid steepest descent method [11] with a simple operator that approximates the convex projection onto the constraint set defined for each quantized image [12], the proposed method minimizes these functions over the feasible set, the set of all images satisfies all quantization constraints. Finally we demonstrate the effectiveness of the proposed method by showing a comparison of images derived from the proposed method, POCS based method, and generalizations of the proposed method to minimize energy of output of Laplacian operator.

A preliminary version of this paper had been presented

Manuscript received April 2, 2007.

Manuscript revised September 3, 2007.

[†]The author is with the Dept. of Electrical Engineering & Computer Science, Nagoya University, Nagoya-shi, 464-8603 Japan.

[††]The authors are with the Dept. of Communications & Integrated Systems, Tokyo Institute of Technology, Tokyo, 152-8552 Japan.

a) E-mail: hasegawa@nuee.nagoya-u.ac.jp

DOI: 10.1093/ietfec/e91–a.2.673

at an international conference [13].

2. Preliminaries

2.1 Notations

Let $\mathbb{R}$ and $\mathbb{Z}$ be the set of all real numbers and integers, respectively. Let $\mathcal{H}$ be a Hilbert space equipped with its inner product $\langle\cdot,\cdot\rangle_{\mathcal{H}}$ and induced norm $\|x\|_{\mathcal{H}}^2 := \langle x, x\rangle_{\mathcal{H}}$, $\forall x \in \mathcal{H}$. A set $C \subset \mathcal{H}$ is convex provided that $\forall \boldsymbol{u}, \boldsymbol{v} \in C$, $\forall \nu \in (0,1)$, $\nu\boldsymbol{u} + (1-\nu)\boldsymbol{v} \in C$. $d_{\mathcal{H}}(\boldsymbol{u}, C) := \min_{\boldsymbol{v}\in C} \|\boldsymbol{u} - \boldsymbol{v}\|_{\mathcal{H}} = \|\boldsymbol{u} - P_C(\boldsymbol{u})\|_{\mathcal{H}}$. Given a nonempty closed convex set $C \subset \mathcal{H}$, the convex projection $P_C : \mathcal{H} \to C$ assigns every $\boldsymbol{u} \in \mathcal{H}$ to the unique point $P_C(\boldsymbol{u}) \in C$ such that $d_{\mathcal{H}}(\boldsymbol{u}, C) := \min_{\boldsymbol{v}\in C} \|\boldsymbol{u} - \boldsymbol{v}\|_{\mathcal{H}} = \|\boldsymbol{u} - P_C(\boldsymbol{u})\|_{\mathcal{H}}$.

Let $g : \mathcal{H} \to \mathbb{R}$ be a continuous convex function. In this case, for every $\boldsymbol{x} \in \mathcal{H}$, there exists a vector $\boldsymbol{t} \in \mathcal{H}$ satisfying $\langle \boldsymbol{y} - \boldsymbol{x}, \boldsymbol{t}\rangle_{\mathcal{H}} + g(\boldsymbol{x}) \le g(\boldsymbol{y})$ $(\forall \boldsymbol{y} \in \mathcal{H})$. Such $\boldsymbol{t} \in \mathcal{H}$ is called a subgradient of g at $\boldsymbol{x} \in \mathcal{H}$. The set of all subgradient of g at $\boldsymbol{x}$ is called subdifferential of g at $\boldsymbol{x}$ and denoted by $\partial g(\boldsymbol{x}) \neq \emptyset$. We often denote a selection of subgradient by $g'(\boldsymbol{x}) \in \partial g(\boldsymbol{x})$ because it is a natural generalization of gradient of g at $\boldsymbol{x}$. Suppose that g has its nonempty level set: $\mathrm{lev}_{\le 0} g := \{\boldsymbol{x} \in \mathcal{H} \mid g(\boldsymbol{x}) \le 0\}$, which is automatically closed convex set. Then a mapping $T_{\mathrm{sp}(g)} : \mathcal{H} \to \mathcal{H}$ defined by

$$T_{\mathrm{sp}(g)}(\boldsymbol{x}) := \begin{cases} \boldsymbol{x} - \frac{g(\boldsymbol{x})}{\|\boldsymbol{t}\|^2}\boldsymbol{t} & (\boldsymbol{x} \notin \mathrm{lev}_{\le 0} g) \\ \boldsymbol{x} & (\boldsymbol{x} \in \mathrm{lev}_{\le 0} g). \end{cases}$$

is called a *subgradient projection* (relative to g). $T_{\mathrm{sp}(g)}$ is a computationally efficient approximation of $P_{\mathrm{lev}_{\le 0} g}$.

2.2 Super-Precision

For all vectors $\boldsymbol{u} := (u_1, \ldots, u_{\mathcal{P}}), \boldsymbol{v} := (v_1, \ldots, v_{\mathcal{P}})$ in a $\mathcal{P}$ dimensional Euclidean space $\mathbb{R}^{\mathcal{P}}$, its inner product and induced norm are respectively defined by $\langle \boldsymbol{u}, \boldsymbol{v}\rangle := \sum_{k=1}^{\mathcal{P}} u_k v_k$ and $\|\boldsymbol{u}\| := \sqrt{\langle \boldsymbol{u}, \boldsymbol{u}\rangle}$. Hereafter for $\boldsymbol{u} := (u_1, \ldots, u_{\mathcal{P}}) \in \mathbb{R}^{\mathcal{P}}$, its m th component u_m is equivalently denoted by $\boldsymbol{u}(m)$. Let M, N, and L be positive integers. Suppose that we have a vector $\boldsymbol{x} \in \mathbb{R}^{L^2 MN}$ and a sequence $(\boldsymbol{y}_k)_{k\in\mathcal{I}:=\{1,2,\ldots,\mathcal{K}\}} \subset \mathbb{R}^{MN}$ derived through lexicographically reordering pixels of an unknown $LM \times LN$ high-resolution images and observed $M \times N$ low-resolution images, respectively. Each low-resolution image is assumed to be generated by :

$$\boldsymbol{y}_k = DH_k\boldsymbol{x} \qquad (k \in \mathcal{I}), \tag{1}$$

where $H_k \in \mathbb{R}^{L^2MN \times L^2MN}$ stands for a degradation such as blur and sub-pixel shifts, and $D \in \mathbb{R}^{MN \times L^2MN}$ changes resolution by averaging each $L \times L$ region. Hereafter we assume that the shifts are sufficiently estimated by registration techniques [1]. The shift can be exactly given if we employ a system in [2, Fig. 8]. In order to focus on compensation of the quantization effect, we also assume that the blur is given or estimated for example by using depth information [14], although the estimation of blur is more difficult than that of the shifts [2]. Then each low-resolution image $\boldsymbol{y}_k$ is quantized after conversion

$$\boldsymbol{z}_k := Q(T_k(\boldsymbol{y}_k)) \qquad (k \in \mathcal{I})$$

where Q is a quantization operator with quantization intervals $(q_m)_{m=1}^{MN}$ such that

$$(Q(\boldsymbol{u}))(m) = q_m \times \left\lfloor \frac{\boldsymbol{u}(m)}{q_m} + \frac{1}{2} \right\rfloor \quad (1 \le m \le MN),$$

and $T_k(\boldsymbol{y}) := S_k(\boldsymbol{y}) + \boldsymbol{t}_k$ is an operator that consists of known linear transformation $S_k : \mathbb{R}^{MN} \to \mathbb{R}^{MN}$ and known constant shifts $\boldsymbol{t}_k \in \mathbb{R}^{MN}$. A typical example of such an operator T_k is the MPEG compression scheme where S_k is the DCT transform and $\boldsymbol{t}_k$ is the motion estimation. If a camera system has a large quantization interval because of limited system capability, it would be the other example such that $T_k = I$. Hereafter we assume that $T_k = I$ and $\boldsymbol{t}_k = \boldsymbol{0}$ for notational simplicity. The latter assumption is justified because $\boldsymbol{t}_k$ is nothing but an offset of the quantization and T_k can be a part of the linear operator DH_k in (1).

Throughout this paper, we consider next problem: *recover $\boldsymbol{x}$ from given quantized data $(\boldsymbol{z}_k)_{k\in\mathcal{I}\subset\mathbb{Z}}$ and sufficiently estimated $(H_k)_{k\in\mathcal{I}}$.*

The first solution is given by Gunturk et al. [3]. First they define constraint sets

$$C_{(k,m,n)} := \{\boldsymbol{x} \in \mathbb{R}^{L^2MN} \mid (QDH_k\boldsymbol{x})(m,n) = \boldsymbol{z}_k(m,n)\}$$

with (m,n) th pixel $\boldsymbol{x}(m,n)$ of the image $\boldsymbol{x}$. Each $C_{(k,m,n)}$ is a halfspace and the convex projection $P_{C_{(k,m,n)}} : \mathbb{R}^{LM\times LN} \to C_{(k,m,n)}$ onto it can be easily computed. Then they characterize the set of all candidates for solutions, which is the set of all images coincide to the observed images $(\boldsymbol{z}_k)_{k\in\mathcal{I}}$ after degradation by the operator QDH_k, as the intersection $\bigcap_{k\in\mathcal{I}}\bigcap_{m=1}^{M}\bigcap_{n=1}^{N} C_{(k,m,n)}$. An image in the intersection is derived as convergent point of the following iterative scheme

$$\boldsymbol{x}_{n+1} = P_{C_{(\mathcal{K},M,N)}} \ldots P_{C_{(1,1,2)}} P_{C_{(1,1,1)}} \boldsymbol{x}_n \qquad (n = 0, 1, \ldots)$$

for any $\boldsymbol{x}_0 \in \mathbb{R}^{LM\times LN}$.

If a large quantization interval q_m is employed for higher compression rate or limitation of sensor ability, the intersection becomes broad in general and includes visually unnatural images. A candidate to avoid selection of such images would be introduction of some additional measurement. Indeed, Elad and Feuer [8] proposed a method to minimize a quadratic function over a data-fidelity set. However, their method can not be applied if the intersection is not simply enough to compute the convex projection onto it (See Appendix). In the next section we present a method that gives a smooth image satisfying all of the given quantization constraints.

Remark 1: In general, image recoveries, especially super-resolution, are severely affected by the estimation error in motion, blur, and noise. The problem considering here is rather robust to the additive noises to the low resolution

images since the large quantization interval is usually employed for the compression, whereas the exact estimations are necessary for motion and blur as assumed in this section. Even if there are some errors in estimation of these parameters, the first assumption in the next section will hold and the considering problem is still valid because the large quantization interval defines broad constraint sets.

3. Proposed Edge-Preserving Super-Precision Subject to Quantization Constraints

Let constraint sets in terms of quantized data $(z_k)_{k\in\mathcal{I}\subset\mathbb{Z}}$ be

$$\begin{aligned} C_k &:= \left\{\boldsymbol{x}\in\mathbb{R}^{L^2MN} \,|\, QDH_k\boldsymbol{x} = z_k\right\} \\ &\equiv \bigcap_{m=1}^{M}\bigcap_{n=1}^{N} C_{(k,m,n)} \neq \emptyset \qquad (k\in\mathcal{I}). \end{aligned}$$

An equivalent expression of each set as a level set is given by

$$\begin{aligned} &\mathrm{lev}_{\le 0}(g_k) \\ &= \left\{\boldsymbol{x}\in\mathbb{R}^{L^2MN} \,\middle|\, g_k(\boldsymbol{x}) := \max_{1\le m\le L^2MN}\{|(DH_k\boldsymbol{x}-z_k)(m)|\} - \frac{q_m}{2} \le 0\right\} \\ &\equiv C_k. \end{aligned}$$

A subgradient projection $T_{\mathrm{sp}(g_k)}$ relative to each g_k is given by the following scheme [12]. Let

$$\begin{aligned} \Psi_k &:= \left\{\boldsymbol{x}\in\mathbb{R}^{L^2MN} \,|\, \left\langle \boldsymbol{x}, (DH_k)^T\Omega_k\boldsymbol{x}\right\rangle \right. \\ &\quad \left. \ge \left\langle P_{DH_kC_k}(DH_k\boldsymbol{x}), \Omega_k\boldsymbol{x}\right\rangle\right\}, \end{aligned}$$

where $DH_kC_k := \{DH_k\boldsymbol{x}\,|\,\boldsymbol{x}\in C_k\} = \{\boldsymbol{u}\in\mathbb{R}^{MN}\,|\,\boldsymbol{u}(m)\in z_k(m)+[-\frac{q_m}{2},\frac{q_m}{2}]\}$, $P_{DH_kC_k}:\mathbb{R}^{MN}\to DH_kC_k$ is the convex projection onto hyper-cuboid DH_kC_k, and

$$\Omega_k\boldsymbol{x} := P_{DH_kC_k}(DH_k\boldsymbol{x}) - DH_k\boldsymbol{x}.$$

Then an operator approximating the convex projection onto C_k given by

$$\begin{aligned} T_{\mathrm{sp}(g_k)}(\boldsymbol{x}) &= P_{\Psi_k}(\boldsymbol{x}) \\ &:= \boldsymbol{x} + \begin{cases} \boldsymbol{0} & \text{if } DH_k\boldsymbol{x}\in C_k, \\ \dfrac{\|\Omega_k\boldsymbol{x}\|^2}{\|(DH_k)^T\Omega_k\boldsymbol{x}\|^2}(DH_k)^T\Omega_k\boldsymbol{x} & \\ & \text{otherwise.} \end{cases} \end{aligned}$$

The set of all candidates for the solution characterized as an intersection

$$\bigcap_{k\in\mathcal{I}} C_k = \left\{\boldsymbol{x}\in\mathbb{R}^{L^2MN} \,\middle|\, \max_{k\in\mathcal{I}} g_k(\boldsymbol{x}) \le 0\right\}.$$

As we stated at the end of previous section, further selection in the intersection to pursue smoothness is necessary. The following differentiable functions are candidates for the measurement of smoothness.

1. **Huber function**
   The objective function to be minimized is

$$\Theta_1(\boldsymbol{x}) := \sum_{m=1}^{LM}\sum_{n=1}^{LN}\sum_{l=1}^{4}\rho((\delta_\ell(\boldsymbol{x}))(m,n))$$

   where a smooth approximation of $|\cdot|$

$$\rho(t) := \begin{cases} t^2 & \text{if } |t|<\alpha \\ 2\alpha|t|-\alpha^2 & \text{otherwise} \end{cases}$$

   with a fixed small $\alpha>0$, and

$$\begin{aligned} (\delta_1(\boldsymbol{x}))(m,n) &:= \boldsymbol{x}(m,n+1) - 2\boldsymbol{x}(m,n) \\ &\quad +\boldsymbol{x}(m,n-1) \\ (\delta_2(\boldsymbol{x}))(m,n) &:= \frac{1}{2}\boldsymbol{x}(m-1,n+1) - \boldsymbol{x}(m,n) \\ &\quad +\frac{1}{2}\boldsymbol{x}(m+1,n-1) \\ (\delta_3(\boldsymbol{x}))(m,n) &:= \boldsymbol{x}(m+1,n) - 2\boldsymbol{x}(m,n) \\ &\quad +\boldsymbol{x}(m-1,n) \\ (\delta_4(\boldsymbol{x}))(m,n) &:= \frac{1}{2}\boldsymbol{x}(m+1,n-1) - \boldsymbol{x}(m,n) \\ &\quad +\frac{1}{2}\boldsymbol{x}(m-1,n+1). \end{aligned}$$

   Note: The above Huber function provides a MRF (Markov Random Field) called Huber MRF, which can be applied to a MAP super-resolution as an image prior [10]. The effect of selection of α, see [10, Fig. 14].
2. **a smooth approximation of total variation**
   A smoothed version of total variation is straightforwardly derived by approximating $|\cdot|$ by ρ

$$\begin{aligned} \Theta_2(\boldsymbol{x}) := \sum_{m=1}^{LM}\sum_{n=1}^{LN}\{&\rho^2(x(m+1,n)-x(m,n)) \\ &+\rho^2(x(m,n)-x(m,n+1))\}^{1/2}, \end{aligned}$$

   where $x(LM+1,n) := x(LM,n)$ $(n=1,\ldots,LN)$ and $x(m,N+1) := x(m,LN)$ $(m=1,\ldots,LM)$, respectively.

These measurements Θ_1 and Θ_2 are smooth convex functions and satisfy a condition so called *edge-preserving* (a function ϕ is called edge-preserving if $\phi(t)<t^2$ as $t\to\infty$ [5]).

Hereafter we propose a method that minimizes the measurements over the intersection. This minimization is resolved by the direct application of the following fact.

Fact 1: (A version of hybrid steepest descent method for quasi-nonexpansive mapping) [11, Prop.6] Assume $\dim(\mathcal{H})<\infty$. Suppose $\Phi:\mathcal{H}\to\mathbb{R}$ is a continuous convex function with $\mathrm{lev}_{\le 0}\Phi\neq\emptyset$. Let Φ' be a selection of the subdifferential $\partial\Phi$ and let Φ' be bounded on any bounded set. Suppose K be a bounded closed convex set such that $\mathrm{lev}_{\le 0}\Phi\cap K\neq\emptyset$. Assume the Gâteau derivative Θ' of $\Theta:\mathcal{H}\to\mathbb{R}$ is κ-Lipschitzian over K, i.e. $\exists\kappa>0$, $\|\Theta'(x)-\Theta'(y)\|\le\kappa\|x-y\|$ for all $x,y\in K$. Then by using any $u_0\in\mathcal{H}$ and any $(\lambda_n)_{n\ge 1}\subset[0,\infty)$ satisfying (H1)

$\lim_{n\to\infty}\lambda_n = 0$ and (H2) $\sum_{n\geq 1}\lambda_n = \infty$, the sequence generated by $u_{n+1} := P_K T_\alpha(u_n) - \lambda_{n+1}\Theta'(P_K T_\alpha(u_n))$ satisfies $\lim_{n\to\infty} d(u_n, \Gamma) = 0$, where $T_\alpha := (1-\alpha)I + \alpha T_{\mathrm{sp}(\Phi)}$ and $\Gamma := \mathrm{arginf}_{\mathrm{lev}_{\leq 0}\Phi\cap K}\Theta(x) \neq \emptyset$ (Note: The iterative scheme does not require the inversion of $\Theta''(x)$ at any $x \in \mathcal{H}$. This is notable advantage of the hybrid steepest descent method because the inversion of $\Theta''(x)$ is often computationally intensive even in a simplest case where Θ is a quadratic function. The necessity of the conditions (H1) and (H2) for $\lim_{n\to\infty} d(u_n, \Gamma) = 0$ is discussed in [11, Remark 1]. The speed of convergence of $(d(u_n, \Gamma))_{n=0}^{\infty}$ can be raised by employing reasonable step sizes $(\lambda_n)_{n\geq 1}$ in the initial stage). □

Algorithm 1: (Proposed Edge-Preserving Super-Precision) Let $\Theta = \Theta_1$ or Θ_2, $T_{\mathrm{sp}(\Phi)} := T_{\mathrm{sp}(g_{k_0})}$ with $k_0 := \mathrm{argmax}_{k\in I} g_k(\boldsymbol{x})$, and $K := [0,\mu]^{L^2MN}$ where μ is given maximum intensity. Apply Fact 1 to derive the unique minimizer $\boldsymbol{x}$ of Θ over $K \cap \bigcap_{k\in I} C_k$. □

Remark 2: As shown in the numerical examples, Θ_1 is suitable for almost smooth images whereas Θ_2 is effective when given image consists of several regions with constant intensities.

4. Numerical Examples

4.1 Recovery from Roughly Quantized Still Images

Example 1. For the image "Lenna" (shown in Fig. A· 1(a)) $\boldsymbol{x} \in (\mathbb{R}\cap[0,255])^{512\times 512}$ ($\mu = 255$ means 8 bits/pixel), we have low-resolution images $(\boldsymbol{y}_k)_{k=1}^{12} \subset (\mathbb{R}\cap[0,255])^{256\times 256}$ by application of mutually different sub-pixel shifts, the 2-D Gaussian blur whose variance is

$$\sigma^2 = \begin{cases} 3.0 & \text{for } \boldsymbol{y}_1,\ldots,\boldsymbol{y}_4 \\ 6.0 & \text{for } \boldsymbol{y}_5,\ldots,\boldsymbol{y}_8 \\ 9.0 & \text{for } \boldsymbol{y}_9,\ldots,\boldsymbol{y}_{12}, \end{cases}$$

and downsampling after averaging each 2×2 region (namely, $L = 2$). Then the low-resolution images are equally quantized with a uniform quantization interval $q_m = 16$ (See Fig. A· 1(b)). This interval means the bit-depth is 3 bits.

Next we recover a high-resolution image by applying the algorithm. In this example, for the function ρ, we empirically employ $\alpha = 3$. In addition to the comparison of the proposed method and the conventinal POCS based method [3] (derived images are shown in Figs. A· 1(d), (e) and Fig. A· 1(c),respectively), we introduce the following differentiable function that stands for smoothness.

3. **energy of output of Laplacian**
   A discrete version of Laplacian is given by $\delta_1(\cdot)+\delta_3(\cdot)$. Being a high-pass filter, minimization of squared output $\Theta_3(\boldsymbol{x}) := \|\delta_1(\boldsymbol{x}) + \delta_3(\boldsymbol{x})\|^2$ will produce smooth image.

The above function Θ_3 violates the condition of edge-preserving whereas Θ_1 and Θ_2 satisfy the condition. It can also be minimized by Algorithm 1 and the derived image is shown in Fig. A· 1(f).

It can be verified that the proposed method provides more smooth images while keeping the edge information compared with the conventional POCS based method. From the viewpoint of PSNR, defined for an original image $\boldsymbol{x}$ and its estimate $\widehat{\boldsymbol{x}}$ by

$$\mathrm{PSNR} := -10\log_{10}\frac{\|\boldsymbol{x}-\widehat{\boldsymbol{x}}\|^2}{255^2L^2MN},$$

minimization of Θ_1 and Θ_2 provides better results than that of Θ_3. Minimization of Θ_2 is slightly better than the other in terms of PSNR, however it seems that the derived image is over-smoothed. Indeed, the face of the woman seems like a plate. On the other hand, with minimization of Θ_1, almost exact recovery is provided for smooth regions, for example the face and the shoulder.

Example 2. For an image of a flag (shown in Fig. A· 2(a)) $\boldsymbol{x} \in (\mathbb{R}\cap[0,255])^{400\times 298}$, similar to the previous example, we have low-resolution images $(\boldsymbol{y}_k)_{k=1}^{12} \subset (\mathbb{R}\cap[0,255])^{200\times 149}$ by applying mutually different sub-pixel shifts, the 2-D Gaussian blur whose variance is

$$\sigma^2 = \begin{cases} 4.0 & \text{for } \boldsymbol{y}_1,\ldots,\boldsymbol{y}_4 \\ 8.0 & \text{for } \boldsymbol{y}_5,\ldots,\boldsymbol{y}_8 \\ 16.0 & \text{for } \boldsymbol{y}_9,\ldots,\boldsymbol{y}_{12}, \end{cases}$$

and quantized low-resolution images are derived where quantization interval $q_m = 16$ (See Fig. A· 2(b)). For the other parameters such as α, we employ the same value as the previous example.

The results are shown in Fig. A· 2. Contrary to the previous example, the original image has clear edges around the characters and the flag. In such a case, as shown in Figs. A· 2(i)–(k) and PSNRs, minimization of Θ_2 is suitable for recovery.

4.2 Recovery from Compressed Movie

As noted in Sect. 2.2, the proposed method can be applied to compressed movies where T_k stands for the motion compensation and the DCT transform. For a sequence of images of a distant view (8th frame is shown in Fig. A· 3(a)) $(\boldsymbol{x}_n)_{n=1}^{8} \subset (\mathbb{R}\cap[0,255])^{192\times 288}$, we have low-resolution images $(\boldsymbol{y}_n)_{n=1}^{8} \subset (\mathbb{R}\cap[0,255])^{96\times 144}$ by applying mutually different sub-pixel shifts, the 2-D uniform Gaussian blur whose variance is $\sigma^2 = 4.0$, DCT after the motion compensation relative to the first frame, and finally quantized low-resolution images are derived where quantization interval $q_m = 16$ (See Fig. A· 3(b)). This interval means bit-depth is 4 bit.

Then with all frames, $\boldsymbol{x}_8$ is estimated by the proposed method as shown in Figs. A· 3(c) and (d). Since the original image consists of several flat regions with clear edges, minimization of Θ_2 provides a better result.

5. Conclusion

In this paper, we proposed a method that recovers a smooth

high-resolution image from several blurred and roughly quantized low-resolution images. We introduced two cost functions to pursue smoothness while keeping edge information. Then it has been shown that iterative operations based on hybrid steepest descent method generate a sequence that converges to an unique minimizer of the cost function over the set of all candidates characterized by observed quantized images. It was verified in the numerical examples that the proposed method provides visually natural images compared with a conventinal POCS-based method and minimization of squared output of Laplacian.

Acknowledgment

The authors would like to express deep gratitude to Prof. K. Sato of Nagoya University for his kind support to this work.

References

[1] S.C. Park, M.K. Park, and M.G. Kang, "Super-resolution image reconstruction — A technical overview," IEEE Signal Process. Mag., vol.20, no.3, pp.21–36, May 2003.
[2] M.K. Ng and N.K. Bose, "Mathematical analysis of super-resolution methodology," IEEE Signal Process. Mag., vol.20, no.3, pp.62–74, May 2003.
[3] B. Gunturk, Y. Altunbasak, and R.M. Mersereau, "Gray-scale resolution enhancement," Proc. IEEE Workshop on Multimedia Signal Processing, pp.155–160, 2001.
[4] Y. Alutunbasak, A.J. Patti, and R.M. Mersereau, "Super-resolution still and video reconstruction from MPEG-coded video," IEEE Trans. Circuits Syst. Video Technol., vol.12, no.4, pp.217–226, April 2002.
[5] C.A. Segall, R. Molina, and A.K. Katsaggelos, "High-resolution images from low-resolution compressed video," IEEE Signal Process. Mag., vol.20, no.3, pp.37–48, May 2003.
[6] C.A. Segall, A.K. Katsaggelos, R. Molina, and J. Mateos, "Bayesian resolution enhancemnet of compressed video," IEEE Trans. Image Process., vol.13, no.7, pp.898–911, July 2004.
[7] H. Stark and Y. Yang, Vector space projections — A numerical approach to signal and image processing, neural nets, and optics, John Wiley & Sons, 1998.
[8] M. Elad and A. Feuer, "Restoration of a single superresolution image from several blurred, noisy, and undersampled measured images," IEEE Trans. Image Process., vol.6, no.12, pp.1646–1658, Dec. 1997.
[9] R. Schultz and R. Stevenson, "A Bayesian approach to image expansion for improved definition," IEEE Trans. Image Process., vol.3, no.3, pp.233–242, May 1994.
[10] D. Capel and A. Zisserman, "Computer vision applied to super resolution," IEEE Signal Process. Mag., vol.20, no.3, pp.75–86, May 2003.
[11] I. Yamada and N. Ogura, "Hybrid steepest descent method for variational inequality problem over the fixed point set of certain quasi-nonexpansive mappings," Numerical Functional Analysis and Optimization, vol.25, no.7/8, pp.619–655, 2004.
[12] H. Hasegawa, T. Ono, I. Yamada, and K. Sakaniwa, "An iterative MPEG super-resolution with an outer approximation of framewise quantization constraint," IEICE Trans. Fundamentals, vol.E88-A, no.9, pp.2427–2435, Sept. 2005.
[13] H. Hasegawa, T. Ohtsuka, I. Yamada, and K. Sakaniwa, "An edge-preserving super-precision for simultaneous enhancement of spacial and grayscale resolutions," Proc. 8th IEEE International Workshop on Multimedia Signal Processing, pp.334–337, Dec. 2006.
[14] D. Rajan, S. Chaudhuri, and M.V. Joshi, "Multi-objective super resolution: Concept and examples," IEEE Signal Process. Mag., vol.20, no.3, pp.49–61, May 2003.

Appendix: Practical Limitation of the Method in [8]

Here we demonstrate a simple example that sequential projections onto two constraint sets and update to steepest descent direction of a cost function, a straightforward generalization of [8], fail to converge to the minimizer over the intersection of these two sets. Let a quadratic cost function with two variable x, y be

$$f(x,y) := \frac{1}{2}\left\{\left(x-\frac{13}{8}\right)^2+\left(y-\frac{\sqrt{3}}{8}\right)^2\right\}.$$

Suppose that we have two halfspaces

$$V_1 := \left\{(x,y)\;\middle|\; y \geq \frac{\sqrt{3}}{3}x\right\}$$
$$V_2 := \left\{(x,y)\;\middle|\; y \leq -\frac{\sqrt{3}}{3}x\right\}.$$

The unique minimizer of f over $V_1 \cap V_2$ is $(0,0)$. For a starting point $(x_0, y_0) := (\frac{3}{8}, -\frac{\sqrt{3}}{8})$, we have

$$(x_0,y_0) - \frac{1}{2}\nabla f|_{(x,y)=(x_0,y_0)} = (1,0)$$
$$P_{V_1}(1,0) = \left(\frac{3}{4}, \frac{\sqrt{3}}{4}\right)$$
$$P_{V_2}\left(\frac{3}{4}, \frac{\sqrt{3}}{4}\right) = (x_0,y_0),$$

where $\frac{1}{2}$ is introduced for convergence of conventional steepest descent methods.

The above equations implies that, even if we combine the steepest descent update and the sequential projections, the generated sequence can not converge to the minimizer of f over $V_1 \cap V_2$. Thus the method in [8] requires further assumption that given closed convex sets can be replaced by its intersection, which is simply enough to compute the convex projection onto it. However, for example, blurring in image recovery provides convex sets with complicated shapes and it is computationally intensive task to derive the convex projection onto their intersection. This means that the method in [8] can not be applied to practical situations in general.

(a) Original image. (8 bits/pixel)

(b) Blurred and quantized image. (3 bit/pixel) (PSNR 26.7 dB)

(c) POCS based method. (PSNR 29.0 dB)

(d) Huber function. (PSNR 29.7 dB)

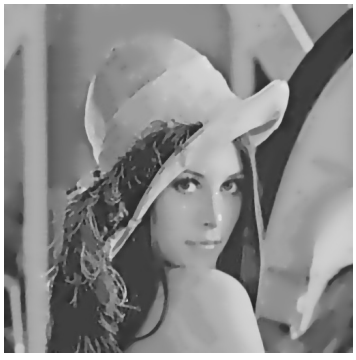

(e) Smoothed total variation. (PSNR 29.9 dB)

(f) Squared output of Laplacian. (PSNR 29.5 dB)

(g) Difference between (a) and (b).

(h) Difference between (a) and (c).

(i) Difference between (a) and (d).

(j) Difference between (a) and (e).

(k) Difference between (a) and (f).

Fig. A· 1 Results and recovery errors (“Lenna”).


(a) Original image. (8 bits/pixel)


(b) Blurred and quantized image. (4 bits/pixel) (PSNR 23.5 dB)


(c) POCS based method. (PSNR 27.9 dB)


(d) Huber function. (PSNR 27.8 dB)


(e) Smoothed total variation. (PSNR 29.2 dB)


(f) Squared output of Laplacian. (PSNR 27.8 dB)


(g) Difference between (a) and (b).


(h) Difference between (a) and (c).


(i) Difference between (a) and (d).


(j) Difference between (a) and (e).


(k) Difference between (a) and (f).

Fig. A· 2 Results and recovery errors (A flag).

(a) Original image. (8 bits/pixel)

(b) Blurred and compressed image. (4 bits/pixel) (PSNR 26.4 dB)

(c) Huber function. (PSNR 30.3 dB)

(d) Smoothed total variation. (PSNR 30.7 dB)

(e) Difference between (a) and (b).

(f) Difference between (a) and (c).

(g) Difference between (a) and (d).

Fig. A· 3 Results and recovery errors (a distant view of Tokyo Bay).

Hiroshi Hasegawa received the B.E., M.E., and D.E. degrees all in Electrical and Electronic Engineering from Tokyo Institute of Technology, Tokyo, Japan, in 1995, 1997, and 2000, respectively. From 2000 to 2005, he was a research associate of the Dept. of Communications and Integrated Systems, Tokyo Institute of Technology. Currently he is an associate professor of Nagoya University. His current research interests include photonic networks, image processing (especially super-resolution), multidimensional digital signal processing and time-frequency analysis. He received the young researcher awards from SITA (Society of Information Theory and its Applications) and IEICE (Institute of Electronics, Information and Communication Engineers) in 2003 and 2005, respectively. Dr. Hasegawa is a member of SITA and IEEE.

Toshinori Ohtsuka received the B.E. and the M.E. degrees from Tokyo Institute of Technology in 2005 and the Tokyo University in 2007, respectively. He is now with NTT Communications. His research interest includes high-speed networking, digital signal processing and image processing, especially super-resolution image recovery.

Isao Yamada received the B.E. degree in computer science in 1985 from University of Tsukuba, Ibaraki, Japan, and the M.E. and Ph.D. degrees in Electrical and Electronic Engineering from Tokyo Institute of Technology, Tokyo, Japan, in 1987 and 1990, respectively. In 1990, he joined the Department of Electrical and Electronic Engineering at Tokyo Institute of Technology, as a research associate, and became an associate professor there in 1994. Currently he is an associate professor in the Department of Communications and Integrated Systems at Tokyo Institute of Technology. From August 1996 to July 1997, he stayed at Pennsylvania State University as a Visiting Associate Professor. His current research interests are in Mathematical/ Multidimensional/ Statistical/ Adaptive/ Array Signal Processing, Image Processing, Optimization Theory, Nonlinear Inverse Problem, Information and Coding Theory and Neural Computing. He received the Excellent Paper Awards, in 1990, 1994 and 2006, and the Young Researcher Award, in 1992, from IEICE, the ICF Research Award in 2004, from ICF and the DoCoMo Mobile Science Award (Fundamental Science Division) in 2005, from MCF (Mobile Communication Fund). Dr. Yamada is a member of the IEEE, AMS, SIAM, JSIAM, and SITA.

Kohichi Sakaniwa received B.E., M.E., and Ph.D. degrees all in electronic engineering from the Tokyo Institute of Technology, Tokyo Japan, in 1972, 1974 and 1977, respectively.He joined the Tokyo Institute of Technology in 1977 as a research associate and served as an associate professor from 1983 to 1991. Since 1991 he has been a professor in the Department of Electrical and Electronic Engineering, and since 2000 in the Department of Communication and Integrated Systems, Graduate School of Science and Engineering, both in the Tokyo Inst. of Tech. From November 1987 to July 1988, he stayed at the University of Southwestern Louisiana as a Visiting Professor. He received the Excellent Paper Award from the IEICE of Japan in 1982, 1990, 1992 and 1994. His research area includes Communication Theory, Error Correcting Coding, (Adaptive) Digital Signal Processing and so on. Dr. Sakaniwa is a member of IEEE, Information Processing Society of Japan, Institute of Image Information and Television Engineers of Japan, and Society of Information Theory and its Applications.